Available online at www.sciencedirect.com
SCIENCE DIRECT®
Journal of Solid State Chemistry 177 (2004) 4098–4103
JOURNAL OF SOLID STATE CHEMISTRY
www.elsevier.com/locate/jssc

Phase transformations in nanocrystalline TiO_2 milled in different milling atmospheres

Xiaoyan Pan, Xueming Ma*

Department of Physics, East China Normal University, Shanghai 200062, People's Republic of China

Received 11 May 2003; received in revised form 9 August 2004; accepted 11 August 2004

Abstract

The structural evolution of nanocrystalline TiO_2 milled in different milling atmospheres was studied by X-ray diffraction (XRD), Raman spectroscopy and X-ray photoelectron spectroscopy. Rietveld refinements of the XRD data showed that high-energy ball milling induced the transformations from anatase to srilankite and rutile at room temperature and ambient pressure. The milling atmospheres with different oxygen partial pressures had an influence on the transformation kinetics of anatase. When the nanocrystalline TiO_2 powders were, respectively, milled in oxygen, air and nitrogen atmospheres, the transformation rates of anatases in turn increased with a decrease in oxygen partial pressure of the milling atmosphere, due to the reducing concentration of oxygen vacancies in the milled TiO_2 lattice.

Keywords: Nanocrystalline TiO_2; Milling atmosphere; Phase transformation

1. Introduction

Mechanical alloying (MA) is an effective technique of synthesizing a variety of materials including nanocrystalline materials, amorphous alloys, intermetallics and supersaturated solid solution alloys [1]. Besides, it has been shown that mechanical milling can induce the structural transformations in solids [1,2]. By this process, many metastable structures existing at high pressure and/or high temperature can even form at room temperature and ambient pressure. During ball milling, powder is subjected to severe deformation, fracture and cold weld, through which nanosized powder particles with high reactivity are produced. Consequently, interactions between powder particles and/or interactions between powder particles and surrounding media are likely to occur. It has been found that the milling atmosphere can change the nature of the powder and has an effect on the constitution, dimension and structural evolution of the milled powder [1–3].

Nanocrystalline TiO_2 has attracted considerable attention in recent years due to its applications in environment protection, protection against ultraviolet irradiation, antibiosis, pigment, optical coatings, etc. TiO_2, a polymorphic material, exists in three crystalline forms in nature: rutile, anatase, brookite and two high-pressure phases: srilankite and TiO_2-III. Some properties of TiO_2 are closely related to its structure. For example, it has been shown that anatase has a higher activity than rutile, while the mixed phase TiO_2 containing small quantities of rutile in anatase exhibits higher photoacitivity than pure anatase TiO_2. Polymorphism in TiO_2 at high pressure is of interest in geophysics because it is possibly a model of the behavior of SiO_2 in the earth's lower mantle [4]. Therefore, the polymorphic transformation in TiO_2 has been extensively studied [5–9]. It has been demonstrated that the anatase–rutile transformation usually takes place at high temperature and the anatase–srilankite transformation occurs under high pressure. However, Ren et al. [10]

*Corresponding author. Fax: +86-21-62576217.
E-mail address: xmma@phy.ecnu.edu.cn (X. Ma).

0022-4596/$ - see front matter © 2004 Elsevier Inc. All rights reserved.
doi:10.1016/j.jssc.2004.08.017

found that high-energy ball milling can trigger the polymorphic transformations in TiO_2 at room temperature and ambient pressure when they studied the structural evolution of the TiO_2 and graphite mixtures milled in an argon atmosphere. In our previous studies, the milling-induced transformations from anatase to srilankite and rutile also were found when nanocrystalline TiO_2 was milled in air atmosphere. The mechanisms of the milling-induced transformations of anatase in nanocrystalline TiO_2 were discussed and the effects of the milling time and the crystallite size of TiO_2 on the transformation of anatase were studied [11,12].

In this paper, nanocrystalline TiO_2 powders were, respectively, milled in oxygen, air and nitrogen atmospheres, the oxygen partial pressures of which in turn increase. The effects of the milling atmospheres with different oxygen partial pressures on the transformation of anatase in nanocrystalline TiO_2 were investigated using X-ray diffraction (XRD), Raman spectroscopy and X-ray photoelectron spectroscopy (XPS).

2. Experimental

Nanocrystralline TiO_2 powders were prepared by a precipitation-sol–gel method. Metatitanic acid, hydrogen peroxide and ammonia were mixed with the molar ratio of 1:6:2 under continuously stirring in an ice–water bath. After a clear solution was formed, a little surfactant was added. After gelation, the samples were filtered, dried at 120 °C and then calcined at 550 °C.

The high-energy ball milling was performed in a planetary ball mill (QM-1SP). As-prepared nanocrystralline anatase TiO_2 powders (with the average crystallite size of 30 nm or so) were milled at 220 rpm for 40 h in oxygen, air and nitrogen atmospheres, respectively. Steel balls (8 mm in diameter) were mixed with the TiO_2 powder at a ball-to-powder weight ratio of 15:1. Prior to ball milling, the vial was evacuated to less than 10 Pa by a mechanical pump and then purged with oxygen and nitrogen of 1 atm, respectively.

The structures of the unmilled and milled powders were examined by a Rigaku D/Max-C X-ray diffractometer with Cu$K\alpha$ radiation ($\lambda = 0.15418$ nm). The XRD patterns were collected in the range of 20–60° with a step size of 0.02°. The XRD data were analyzed by the Rietveld refinement program FullProf.2k (Version July 2001) [13] based on the structure model of TiO_2 listed in the Joint Committee on Powder Diffraction Standard card (JCPDS card Nos. 21-1272, 21-1276 and 23-1446 for anatase, rutile and srilankite, respectively).

Measurements of Raman spectra were performed on a Super LabRam micro-Raman spectrometer under a backscattering geometry. The excitation source employed was a helium–neon laser operating at 632.8 nm with an average output power of 13 mW. The spectra resolution was set at 2 cm^{-1}.

X-ray photoelectron spectra were recorded using a Perkin-Elmer PHI5000C ESCA system with a 250W Al$K\alpha$ source (1486.6 eV). The powder was pressed to a disc and degassed in the pretreatment chamber before it was removed to the test chamber for XPS analysis. High-resolution spectra were obtained at pass energy of 93.9 eV with a scan step of 0.2 eV. The reference energy used for calibration was the C1*s* signal at a binding energy of 284.6 eV.

3. Results

3.1. X-ray diffraction

XRD patterns for the unmilled and milled nanocrystalline TiO_2 are shown in Fig. 1. The solid dots represent the experimental data points and the continuous curve through the dots represents the refined pattern. The difference between experimental and fitted patterns is shown as continuous line under the individual diffraction pattern. The vertical bars at the bottom of the figure indicate the diffraction peak positions of different TiO_2 phases. It can be seen that the starting nanocrystalline TiO_2 is anatase. However, the reflections of srilankite and rutile besides those of anatase are detected in the nanocrystalline TiO_2 milled in oxygen, air and nitrogen atmospheres, which indicated that ball milling induces

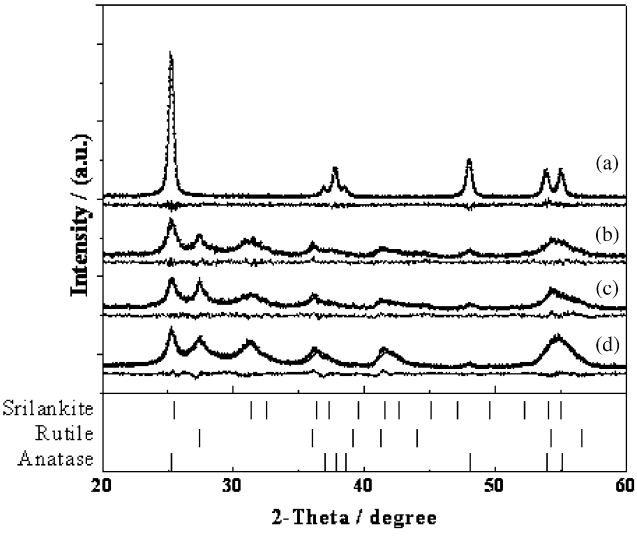

Fig. 1. XRD patterns of nanocrystalline TiO_2 (a) unmilled and milled in (b) oxygen, (c) air and (d) nitrogen. The solid dots correspond to the experimental data points and the continuous curve through the dots represents the refined pattern. The continuous line under the individual diffraction pattern is the difference between experimental and fitted patterns. The diffraction peak positions of different TiO_2 phases are shown as vertical bars at the bottom of the figure.

Table 1
Results of rietveld refinements of XRD data for unmilled and milled nanocrystalline TiO_2

Sample	Weight fraction of anatase (%)	R_p	R_{wp}	S
Unmilled TiO_2	100.00 (0.00)	6.58	10.3	1.14
Oxygen-milled TiO_2	18.72 (0.00)	9.24	11.8	1.21
Air-milled TiO_2	15.17 (0.00)	9.53	12.3	1.26
Nitrogen-milled TiO_2	10.49 (0.00)	7.96	10.4	1.23

R_p, R_{wp} and S are indices of measuring the quality of Rietveld refinement. R_p: profile factor, R_{wp}: weighted profile factor and S: goodness-of-fit indicator.

the phase transformations from anatase to srilankite and rutile in the nanocrystalline TiO_2.

From the plots of the difference between experimental and fitted patterns, it is clearly evident that the experimental patterns have been fitted well. Furthermore, the quality of the agreement between experimental and fitted profiles can be measured by agreement factors: R_p (profile factor), R_{wp} (weighted profile factor) and S (goodness-of-fit indicator) [13]. As shown in Table 1, the lower R factors and the value of S approaching 1.0 confirm the good quality of refinement [14]. The phase amount in the milled nanocrystalline TiO_2 can be determined by the Rietveld method [13]. The weight fractions of anatases are listed in Table 1. It is very clear that the transformation rates of anatases in turn increased when the nanocrystalline TiO_2 powders were milled in oxygen, air and nitrogen atmospheres.

3.2. Raman spectra

As shown in Fig. 2(a), the Raman bands of the unmilled nanocrystalline TiO_2, located at 146, 196, 396, 517 and 636 cm^{-1}, are attributed to anatase [15]. Raman spectra of the nanocrystalline TiO_2 milled in air and nitrogen atmospheres are shown in Figs. 2(b) and (c), respectively. It can be found that some weak Raman bands form at 200–400 cm^{-1}, which correspond to srilankite [9] and some Raman bands become broad and asymmetric envelopes, which suggest the overlaps of bands. As shown in Fig. 3, the Raman envelopes are decomposed with multiple Lorentzian functions. It can be seen that in the Raman spectra of the air-milled nanocrystalline TiO_2, the weak bands of anatase at 398, 514 and 635 cm^{-1} still can be identified besides the strong band at the lowest frequency. However, in the nitrogen-milled nanocrystalline TiO_2, Raman bands of anatase apparently weaken, as indicated by no other Raman bands of anatase but its lowest frequency band, and those of srilankite and rutile strengthen. Therefore, it also can be concluded from Raman spectra that the transformation rate of anatase in the nitrogen-milled TiO_2 is greater than that in the air-milled TiO_2.

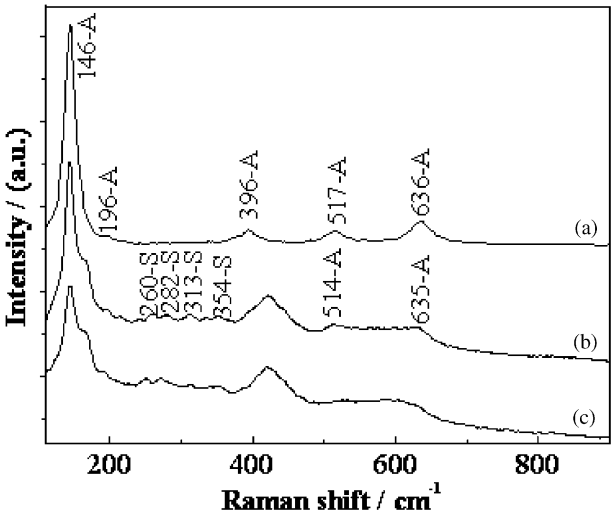

Fig. 2. Raman spectra of nanocrystalline TiO_2 (a) unmilled and milled in (b) air and (c) nitrogen (A and S stand for anatase and srilankite, respectively.)

3.3. X-ray photoelectron spectra

The O1s core level XPS spectra from the TiO_2 powders milled in air and nitrogen atmospheres are, respectively, shown in Figs. 4(a) and (b). The decomposition of the O1s spectrum of the air-milled powder reveals three components at the binding energies of 529.5 ± 0.3, 531.0 ± 0.1 and 532.5 ± 0.4 eV. The components at 529.5 ± 0.3 and 531.0 ± 0.1 eV are unambiguously attributed to the Ti^{4+}–O and Ti^{3+}–O bonds. The 532.5 ± 0.4 eV component can be attributed to hydroxyl group or adsorbed H_2O [16,17]. However, for the O1s spectrum of the nitrogen-milled powder, a contribution at 528.6 ± 0.2 eV had to be added to produce a better fit of the spectrum. This contribution is attributed to the Ti^{2+}–O bond [16]. This suggests that more oxygen vacancies are produced in the nitrogen-milled TiO_2 powder.

As shown in Fig. 5, the N1s spectrum for the air-milled TiO_2 powder can be decomposed into two components at 399.7 ± 0.3 and 401.5 ± 0.4 eV, which are attributed to the molecularly chemisorbed γ-N_2 [18,19]. The N1s spectrum for the nitrogen-milled powder, which can be decomposed into two components at 399.8 ± 0.1 and 401.7 ± 0.3 eV, is almost identical to that of the air-milled powder. Therefore, it is indicated that the TiO_2 powders milled in air and nitrogen atmospheres adsorb a small amount of nitrogen.

4. Discussion

During ball milling, the refinement of the powder particles, availability of large surface area, formation of new fresh surfaces, and variable defects such as

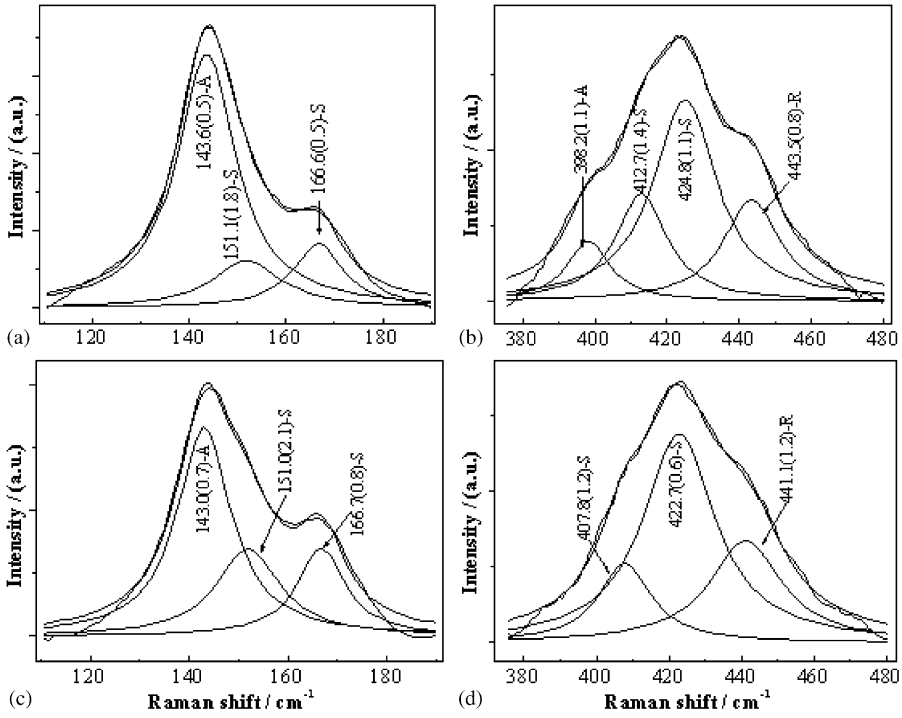

Fig. 3. Fitting of Raman bands of nanocrystalline TiO_2 milled in (a, b) air and (c, d) nitrogen (A, S and R stand for anatase, srilankite and rutile, respectively.)

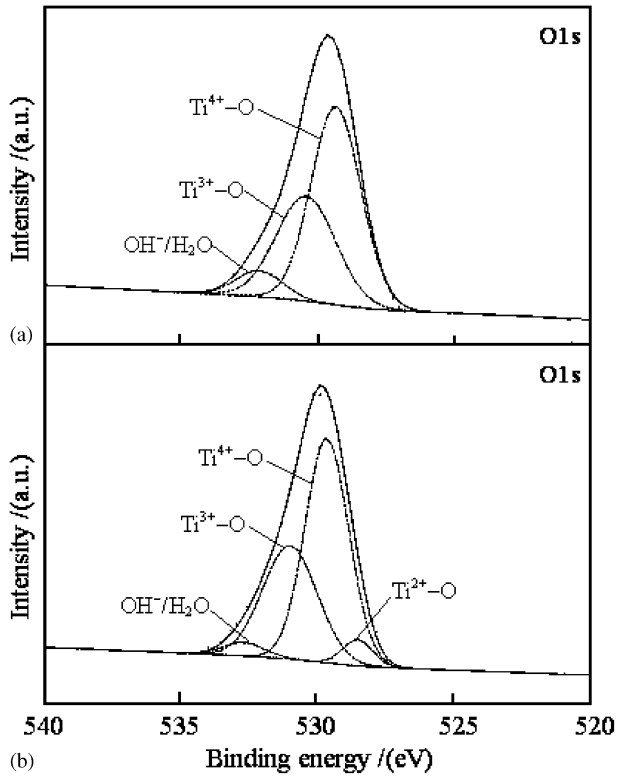

Fig. 4. The O1*s* spectra of nanocrystalline TiO_2 milled in: (a) air and (b) nitrogen.

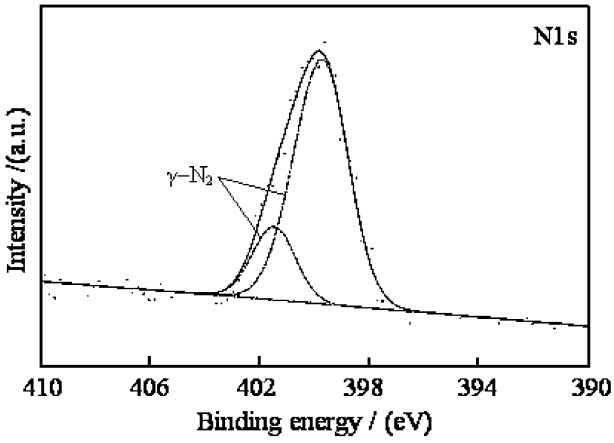

Fig. 5. The N1*s* spectra of nanocrystalline TiO_2 milled in air.

dislocations, vacancies and microcracks, all contribute to trapping gas in the milled powder [1] through physisorption, chemisorption and dissociative chemisorption [20]. Since the milling temperature is much higher than the boiling point of nitrogen, physisorption of nitrogen plays a minimal role in the nitrogen-trapping process. Dissociative chemisorption of nitrogen is negligible, because ball milling cannot supply considerable energy needed for the decomposition from nitrogen molecule to N atom [20]. Moreover, XPS analysis shows

that no peaks at 396 and 397.2 eV assigned to atomic β-N and TiN [18,19] but the peaks corresponding to the molecularly chemisorbed γ-N_2 is detected in the N1s spectra. Therefore, chemisorption of nitrogen molecule on the surfaces of the TiO_2 particles is expected to be dominant and the solid solution of nitrogen atom in TiO_2 lattice and the formation of TiN are not considered.

It has been shown that the local temperature rise and the impact pressure at the collision sites of the powder and the balls, as well as an additional energy due to the grain refinement, defects and the lattice distortion, contribute the milling-induced transformations from anatase to srilankite and rutile [21]. The average impact pressure on the contacting surfaces, P_{max}, and the local temperature rise, ΔT, can be calculated through Eqs. (1) and (2), respectively,

$$P_{max} = 0.4646 v_b^{0.4} (9.8\rho_b/E)^{0.2} E, \quad (1)$$

$$\Delta T = \rho_b v_s v_b^2 (\Delta t/\pi K_0 \rho_P C_P)^{1/2}, \quad (2)$$

where ρ_b, E and v_b are the density, the elastic modulus and the precollision relative velocity of the balls, respectively; v_s is the velocity of a longitudinal wave in the balls; ρ_P, K_0 and C_P are the density, the thermal conductivity and the special heat of the powder, respectively; and Δt is the impact time (see Ref. [21] of the details). In our case, the other milling parameters are identical except for the milling atmosphere. Thus, the local temperature rise and the impact pressure experienced by the powders milled in oxygen, air and nitrogen atmospheres were roughly estimated to be the same. The local temperature rise and the impact pressure are, respectively, 425 °C and 8.08 GPa, which, plus the additional energy, can satisfy the limits of the transformations from anatase to srilankite and rutile [21]. Therefore, the polymorphic transformation of anatase in the nanocrystalline TiO_2 powders can be triggered by ball milling.

It has been proposed that the removal of oxygen ions, which generate oxygen vacancies, accelerates the anatase–rutile transformation and titanium interstitial inhibits it, because the transformation involves an overall contraction of the oxygen structure, as indicated by shrinkage of volume, and breaking of two of the six Ti–O bonds [5]. Many studies have demonstrated that the anatase–rutile transformation kinetics depends on the impurities and the reaction atmosphere, due to the formation of the different lattice defects [5–8]. The presence of lattice defects in the milled TiO_2 powders cannot be excluded and must have an influence on the kinetics of the milling-induced transformation in nanocrystalline TiO_2. Since the densities of anatase, srilankite and rutile are, respectively, 3.893, 4.342, and 4.250 g/cm^3 (which derive from JCPDS cards), the milling-induced the transformations from anatase to srilankite and rutile involve shrinkage of volume. Therefore, an increase in oxygen vacancies can accelerate the milling-induced transformation of anatase in TiO_2.

During ball milling, partial Ti–O bonds on the TiO_2 surface layer may be broken due to mechanical activation and oxygen is released from the TiO_2 lattice. As a result, oxygen vacancies are produced in the TiO_2 lattice. This process can be described by the following reactions:

$$TiO_2 = TiO_{2-x} \ldots xO \text{ (rupture of Ti}-\text{O bonds)}$$

$$TiO_{2-x} \ldots xO = TiO_{2-x} + V_O + (x/2)O_2$$

(formation of oxygen vacancies V_O)

Obviously, kinetic considerations suggest that oxygen partial pressure of the milling atmosphere may have an influence on the concentration of oxygen vacancies in the TiO_2 lattice. The milling atmosphere with low oxygen partial pressure favors the formation of oxygen vacancies and consequently accelerates the milling-induced transformation of anatase. Thus, in the nanocrystalline TiO_2 powders milled in oxygen, air and nitrogen atmospheres, the transformation rates of anatases are different although the local temperature and the impact pressure experienced by the powders are the same. More oxygen vacancies form in the nitrogen-milled TiO_2 powder due to lower oxygen partial pressure, which enhance the transformation of anatase. Because an oxygen atmosphere is not beneficial to the production of oxygen vacancies and less oxygen vacancies form in the TiO_2 lattice, the transformation rate of anatase in the oxygen-milled powder is distinctly slowed down.

5. Conclusions

The transformations from anatase to srilankite and rutile were induced at room temperature and ambient pressure when the nanocrystalline TiO_2 powders were milled in oxygen, air and nitrogen atmospheres. The transformation rate of anatase is dependent on the milling atmosphere. The transformation rates of anatases milled in oxygen, air and nitrogen atmospheres in turn accelerate with a decrease in oxygen partial pressure of the milling atmosphere, due to the reducing concentration of oxygen vacancies in the milled TiO_2 lattice.

References

[1] C. Suryanarayana, Prog. Mater. Sci. 46 (2001) 1–184.
[2] W.A. Kaczmarek, B.W. Ninham, IEEE Trans. Magnet. 30 (1994) 732–734.
[3] Z.H. Chan, T.P. Perng, Appl. Phys. Lett. 70 (1997) 2380–2382.
[4] L.G. Liu, Science 199 (1978) 422–425.

[5] R.D. Shannon, J.A. Pask, J. Am. Ceram. Soc. 48 (1965) 391–398.
[6] K.J.D. MacKenzie, Trans. J. Br. Ceram. Soc. 74 (1975) 121–125.
[7] J.A. Gamboa, D.M. Pasquevich, J. Am. Ceram. Soc. 75 (1992) 2934–2938.
[8] M.K. Akhtar, S.E. Pratsinis, S.V.R. Mastrangelo, J. Am. Ceram. Soc. 75 (1992) 3408–3416.
[9] J.F. Mammone, M. Nicol, S.K. Sharma, J. Phys. Chem. Solids 42 (1981) 379–384.
[10] R.M. Ren, Z.G. Yang, L.L. Shaw, J. Mater. Sci. 35 (2000) 6015–6026.
[11] X.Y. Pan, X.M. Ma, Mater. Lett. 58 (2004) 513–515.
[12] X.Y. Pan, Y. Chen, X.M. Ma, L.H. Zhu, J. Am. Ceram. Soc. 87 (2004) 1164–1166.
[13] J. R. Carvajal, FullProf program is available on the WWW at http://www.ccp14.ac.uk/.
[14] H. Dutta, P. Sshu, S.K. Pradhan, M. De, Mater. Chem. Phys. 77 (2003) 153–164.
[15] T. Oksaka, F. Izumi, Y. Fujiki, J. Raman, Spectroscopy 7 (1978) 321–324.
[16] P.M. Kumar, S. Badrinarayanan, M. Sastry, Thin Solid Film 358 (2000) 122–130.
[17] I. Milosev, H.-H. Strehblow, B. Navinsek, M. Metikos-Hukovic, Surf. Interface Anal. 23 (1995) 529–539.
[18] N.C. Saha, H.G. Tompkins, J. Appl. Phys. 72 (1992) 3072–3079.
[19] R. Asahi, T. Morikawa, T. Ohwaki, K. Aoki, Y. Taga, Science 293 (2001) 269–271.
[20] L.L. Shaw, Z.G. Yang, R.M. Ren, Mater. Sci. Eng. A 244 (1998) 113–126.
[21] X.Y. Pan, Y. Chen, X.M. Ma, L.H. Zhu, Trans. Nonferrous Metals Soc. 13 (2003) 271–275.